ELSEVIER

Applied Catalysis A: General 116 (1994) 237–257

applied catalysis A

Activity-enhanced copper–zinc based catalysts for the hydrogenolysis of esters

Frank Th. van de Scheur[a], Danny S. Brands[a], Bart van der Linden[a], Christian Oude Luttikhuis[a], Eduard K. Poels[a], Leendert H. Staal[a,b,*]

[a]*Department of Chemical Engineering, University of Amsterdam, Nieuwe Achtergracht 166, 1018 WV Amsterdam, Netherlands*

[b]*Unipath Ltd., Norse Road, Bedford MK41 OQG, UK*

(Received 3 March 1994; accepted 6 April 1994)

Abstract

For silica-supported copper–zinc catalysts, a fivefold enhancement of the activity in the hydrogenolysis of methyl acetate has been obtained by high-temperature reductions in the range between 550 K and 700 K. Furthermore, simultaneously, the selectivity was significantly improved. At equal conversion of methyl acetate, catalysts reduced at high temperature make less side products than catalysts reduced at low temperature. The selectivities to methane and ethane as a function of the reduction temperature indicate that these side products are formed on copper metal sites. The formation of ethene most likely proceeds by dehydration of ethanol on acid sites. The presence of copper crystallites in the range of 3–5 nm and the absence of crystalline zinc oxide were established by X-ray diffraction. The activity increase is ascribed to the formation of additional highly active copper sites in interaction with the zinc-containing phase. Fourier-transform infrared spectroscopy of adsorbed carbon monoxide confirmed that metallic copper is more important in the activity than oxidized copper. Reduction at 750 K results in brass formation and catalyst deactivation by evaporation of zinc. The enhanced catalyst activity can be preserved by passivation and is therefore relevant to practical applications. After passivation and prolonged exposure to air the original high activity can be restored by low-temperature reduction.

Keywords: Activity; Carbon monoxide; Copper; Ethane; Ethene; Fourier-transform infrared spectroscopy; Methane; Methyl acetate; Nitrous oxide; Passivation; Reduction; Selectivity; Silica; X-ray diffraction; Zinc

1. Introduction

The synthesis of fatty alcohols by hydrogenolysis of fatty acid methyl esters is characterized by severe process conditions and long residence times in the reactor.

*Corresponding author. Tel. (+44-234) 347161, fax. (+44-234) 218781.

SSDI 0926-860X(94)00079-7

With currently available catalysts, the choice of the reaction temperature is confined to a window ranging from 473 K to 573 K. Thermodynamics dictate that under these conditions elevated pressures are needed to obtain a complete ester conversion [3]. More active catalysts operating at lower temperatures would enable a decrease of the process pressure. Furthermore, the selectivity is critically dependent on the temperature and the properties of the catalyst. In an industrial process, the selectivity is of even more importance than the catalyst activity, as hydrocarbons formed by side reactions cannot economically be separated from the main product, a mixture of fatty alcohols of different chain lengths.

Most currently available catalysts for fatty alcohol synthesis are based on copper chromite, but there is a search for alternatives for chromium as a promoter [2]. Preceding parts of our work [4] have demonstrated that the activity of silica-supported copper catalysts in the hydrogenolysis of esters can be improved by a factor of three by the addition of a zinc promoter. Interesting parallels can be drawn with the methanol synthesis. The activity increase as a result of zinc addition was observed at a reduction temperature of 600 K. The influence of the zinc promoter on the catalyst's reducibility was apparent and is therefore subject for further study. This work deals with the remarkable effects of high-temperature reductions up to 750 K on the activity and selectivity of the silica-supported copper–zinc catalyst. The hydrogenolysis of methyl acetate has been taken as a model reaction.

2. Experimental

2.1. Catalyst preparation and copper metal assay

A silica-supported catalyst containing 15 wt.-% of copper and 7 wt.-% of zinc was prepared by homogeneous precipitation of copper(II) nitrate trihydrate and zinc(II) nitrate tetrahydrate (Merck) onto a fume silica (Degussa Aerosil 200), according to a procedure described in the preceding paper [4]. The metal loadings of the catalyst have been determined by inductively coupled plasma-atom emission spectrometry (ICP/AES).

2.2. Activity measurements

A catalyst system was subjected to a program of subsequent in-situ reductions and activity measurements, as is schematically depicted in Fig. 1. About 300 mg of catalyst, sieve fraction 125–212 μm, was mounted into a U-tube Pyrex glass reactor with an inner diameter of 5 mm. The sample was calcined in 1 $cm^3\ s^{-1}$ of air, with a temperature program of 0.02 $K\ s^{-1}$ to 750 K, followed by a dwell time of twelve hours, and subsequently cooled down to room temperature. Reductions were carried out in a stream of 1 $cm^3\ s^{-1}$ of hydrogen (Praxair 99.999%). The

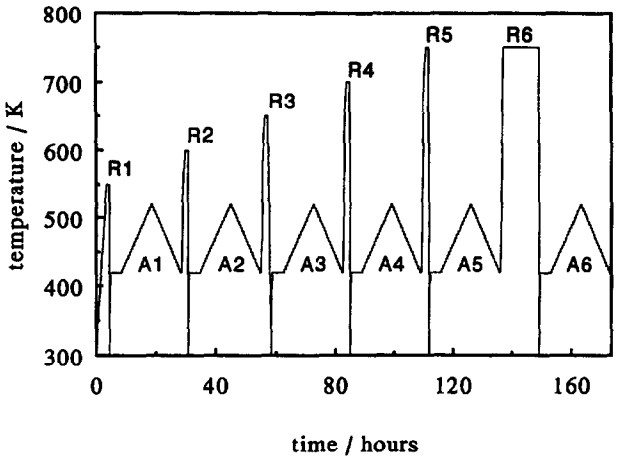

Fig. 1. Program of consecutive reduction and reaction temperature profiles. R1–R6: reductions; A1–A6: activity measurements.

temperature programs of the six reduction steps were conducted as follows (see also Fig. 1):

— step R1: 0.02 K s^{-1} to 550 K, dwell time 1 h;
— step R2: 0.1 K s^{-1} to 550 K, 0.02 K s^{-1} to 600 K, dwell time 1 h;
— step R3: 0.1 K s^{-1} to 600 K, 0.02 K s^{-1} to 650 K, dwell time 1 h;
— step R4: 0.1 K s^{-1} to 650 K, 0.02 K s^{-1} to 700 K, dwell time 1 h;
— step R5: 0.1 K s^{-1} to 700 K, 0.02 K s^{-1} to 750 K, dwell time 1 h;
— step R6: 0.1 K s^{-1} to 750 K, dwell time 12 h.

As is shown in Fig. 1, a cycle of activity measurements was performed after each reduction step. In the activity measurements, the feed to the reactor consisted of a mixture of 0.25 vol.-% of methyl acetate, 10 vol.-% hydrogen and nitrogen as the balance, at a flow-rate of 2 cm^3 NTP s^{-1} and an absolute pressure of 4 bar. The W/F was $1.5 \cdot 10^3$ kg cat. s mol^{-1}. The reaction temperature was cycled between 410 K and 520 K at steps of 5 K and the isothermal stabilization time between two subsequent samples was 30 min. Gas samples were taken by an automatic valve and analyzed on a Chrompack 438A gas chromatograph equipped with a stainless steel Hayesep S column (diameter $^1/_8$ in., length 2 m) and a flame ionization detector (FID). Relative response factors were in agreement with those published by Ackman [5].

2.3. *Thermogravimetric analysis and copper surface area measurements*

Specific copper surface areas were determined according to a method described by Luys et al. [6]. About 300 mg of catalyst precursor was placed in a porous basket in a Setaram TG85 thermobalance. The sample was calcined in a flow of 2 cm^3 s^{-1} of air, heated at a rate of 0.02 K s^{-1} to 750 K, followed by a dwell time of twelve hours and subsequently cooled down to room temperature. Reductions were performed in a flow of 2 cm^3 s^{-1} 67% H_2/33% Ar, according to a schedule

virtually equal to the one applied in the activity measurements. In the first reduction step, the sample was heated at rate of 0.02 K s^{-1} to 500 K, followed by a dwell time of one hour. Succeeding reduction steps were conducted at 650 K for one hour, at 700 K for one hour, at 750 K for one hour and at 750 K for twelve hours. After each reduction step, this sequence was interrupted for a nitrous oxide chemisorption experiment. The thermobalance was evacuated for 15 min at the reduction temperature prior to cooling down to 363 K in an argon flow of 2 cm^3 s^{-1}. Subsequently the gas flow was changed to 2 cm^3 s^{-1} 1% N_2O/99% Ar and the weight increase was monitored until a plateau had been reached. The amount of surface oxygen was determined by extrapolation of the sub-surface contribution to $t=0$. Assuming an adsorption stoichiometry $Cu_s/O_{ads}=2$ and a value of $1.46 \cdot 10^{19}$ Cu_s atoms m^{-2} [7], the copper surface areas could be calculated. The relative experimental error in the calculated values is estimated at 15%.

2.4. X-ray diffraction

In a glass reactor, samples of about 50 mg of the $Cu/ZnO/SiO_2$ catalyst (sieve fraction 38–53 μm) were calcined in a flow of 0.5 cm^3 s^{-1} of air at a temperature of 750 K for 12 h. Reduction was performed in a hydrogen flow of 0.5 cm^3 s^{-1} (Praxair 99.999%) and the heating rates were 0.02 K s^{-1}. For the three samples, different temperature profiles were applied during the reduction: the first was reduced at 600 K for one hour, the second at 700 K for one hour or at 750 K for twelve hours. After the reduction the reactor was purged with helium (Praxair 99.9999%) at room temperature. The catalyst grains were transferred to an X-ray capillary (Hilgenberg, diameter 0.3 or 0.5 mm) attached to the glass reactor, which was subsequently sealed and separated from the reactor under exclusion of air. X-ray measurements were conducted with Cu Kα radiation (0.15418 nm) on a Philips PW1380 diffractometer. Crystallite sizes were calculated using the Scherrer equation with a shape factor 1. The obtained dimensions were corrected for instrumental broadening.

2.5. Hydrogen chemisorption

The experiments were performed in a glass vacuum system for chemisorption equipped with a turbo-molecular pump by which a base pressure of 0.1 mPa could be attained. About 400 mg of catalyst precursor was placed between two plugs of quartz wool in a 20.6 cm^3 Pyrex glass reactor suitable for pretreatment and adsorption. Samples were pretreated in-situ by a calcination in 0.5 cm^3 s^{-1} of air, with a temperature program of 0.02 K s^{-1} to 750 K and a dwell time of four hours. Reductions were carried out in a hydrogen flow of 0.5 cm^3 (Praxair 99.9999%). In the first reduction step the sample was heated at 0.02 K s^{-1} to 600 K, followed by a dwell time of one hour. Using the same sample, subsequent reduction steps were performed in analogy with the program applied in the activity measurements.

After each step, the reduction sequence was interrupted for a hydrogen chemisorption measurement. The reactor was evacuated at the reduction temperature for one hour and cooled down to ambient temperature under vacuum. Adsorption of hydrogen was conducted by expansion of 100 kPa of hydrogen (Praxair 99.9999%) from a glass chamber (31.1 cm^3) to the evacuated reactor. Activation of hydrogen was performed by heating at 0.1 K s^{-1} to 500 K for 30 min. After cooling down to 295 K, the isotherm was measured in the desorption mode. The measured amount of chemisorbed hydrogen could usually be reproduced within 10%, after evacuation at the reduction temperature for one hour.

2.6. *Fourier-transform infrared spectroscopy*

For the preparation of an IR-transparent pellet, 10 mg of finely mortared catalyst powder was pressed at 125 MPa in a 10 mm die. The pellet was mounted in an in-situ infrared cell described by Bijsterbosch [8]. In-situ calcination was conducted in a 1 cm^3 s^{-1} flow of synthetic air (Praxair 99.999%) by heating at 0.02 K s^{-1} to 750 K, with a dwell time of eight hours. The sample was subjected to a sequence of four reduction treatments in a hydrogen flow of 1 cm^3 s^{-1} (Praxair 99.9999%). In the first reduction step, the sample was heated 0.02 K s^{-1} to 600 K, followed by a dwell time of one hour. Subsequent reductions were conducted at 700 K for one hour, 750 K for one hour and 750 K for twelve hours.

After each reduction step, this sequence was interrupted for the adsorption of carbon monoxide. The reduced sample was evacuated at 600 K for 30 min and then cooled down to room temperature under vacuum. The vacuum pressure was lower than 0.01 mPa. Subsequently, 2 kPa of carbon monoxide (Praxair 99.997%) was admitted to the sample cell at room temperature. Fourier-transform infrared (FT-IR) spectra were recorded on a Biorad FT-60A spectrometer, with 256 scans in the range 200–4000 cm^{-1}, at a resolution of 2 cm^{-1}. After five minutes of exposure, the carbon monoxide adsorption spectrum was recorded. Subsequently, the carbon monoxide was removed and evacuation spectra were recorded at a pressure lower than 1 mPa.

3. Results

3.1. *Activity measurements*

The effect of the reduction temperature on the performance of a 15 wt.-% Cu/9 wt.-% ZnO/SiO_2 catalyst is shown in Fig. 2. Starting at 550 K, substantial activity increases are observed up to a reduction temperature of 700 K. A further increase of the reduction temperature results in a decrease of the activity.

A wide range of products is formed in the hydrogenolysis of methyl acetate, but the amounts of methane, ethane and ethene are the most representative of the overall catalyst selectivity.

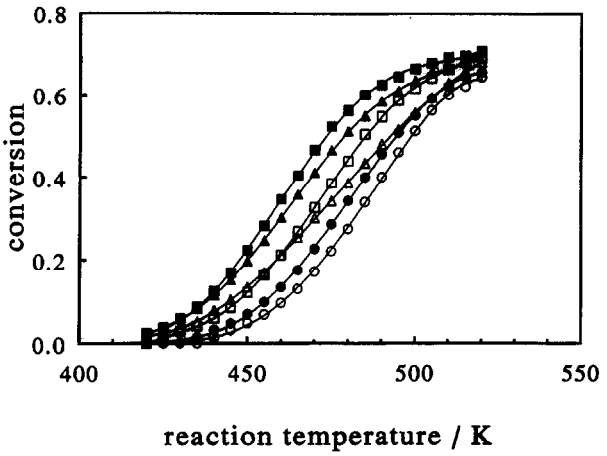

Fig. 2. The activity of a 15 wt.-% Cu/9 wt.-% ZnO/SiO_2 catalyst in the hydrogenolysis of methyl acetate, as a function of the reaction temperature, at varying reduction temperature. (○) T_{red} 550 K, 1 h; (●) T_{red} 600 K, 1 h; (□) T_{red} 650 K, 1 h; (■) T_{red} 700 K, 1 h; (▲) T_{red} 750 H, 1 h; (△) T_{red} 750 K, 12 h.

The definition of C_2-selectivity is equal to the one applied in ref. [4] and is based on the products containing two-carbon fragments:

$$S_i = \frac{\nu_i n_i}{n_{\text{ethene}} + n_{\text{ethane}} + n_{\text{ethanal}} + n_{\text{ethanol}} + 2n_{\text{diethyl ether}} + 2n_{\text{ethyl acetate}}}$$

in which i is one of the products ethene, ethane, ethanal, ethanol, diethyl ether and ethyl acetate; n_i is the amount of product i; ν_i is the stoichiometric coefficient, (2 for diethyl ether and ethyl acetate, 1 for other products). The balance in the denominator corresponds with the amount of methyl acetate reacted. The selectivity to methane is not incorporated in this definition, but is expressed as the C_1-selectivity, given by the amount of methane formed divided by the amount of methyl acetate reacted.

The selectivities to methane, ethane and ethene are presented in the Figs. 3a–3b, 4a–4b and 5a–5b, respectively. These figures relate to the profiles of the methyl acetate conversion versus temperature in Fig. 2. The selectivity has been examined as a function of the reaction temperature and as a function of the conversion of methyl acetate. The latter way of graphical presentation provides insight in the *effective* selectivity, which enables to determine the effect of the pretreatment at a given conversion of methyl acetate.

3.2. Methane formation

For different reduction temperatures, the methane selectivity has been studied as a function of the reaction temperature. This is shown in Fig. 3a. As a general feature, the methane selectivity increases with increasing reaction temperature. For reduction temperatures up to 650 K, the methane selectivity is only a function of the reaction temperature; the amount of methane formed is proportional to the amount

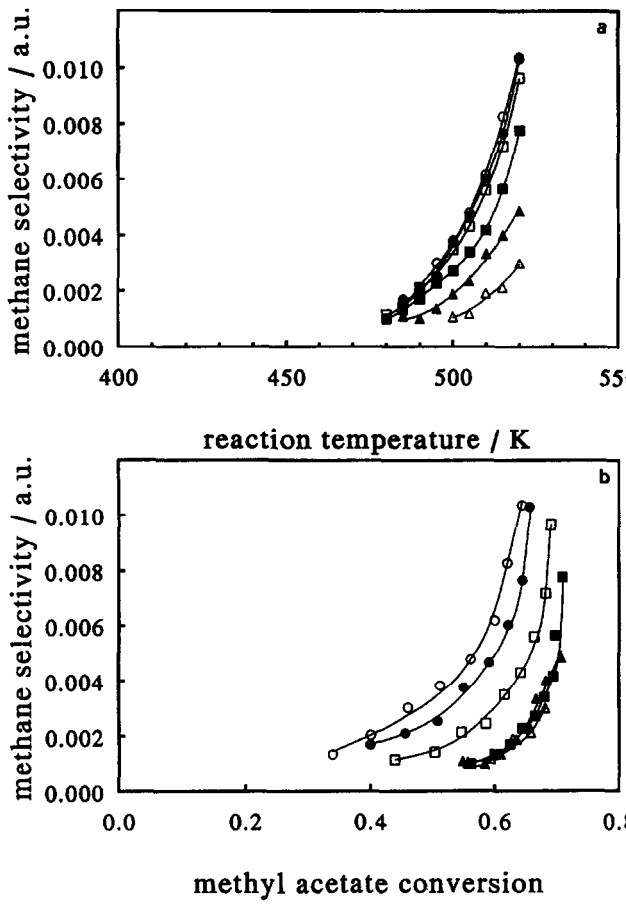

Fig. 3. (a) Effect of the reductive pretreatment. Methane selectivity at varying reduction pretreatment versus the reaction temperature. (b) Effect of the reductive pretreatment. Effective methane selectivity at varying reduction pretreatment versus the methyl acetate conversion. (○) T_{red} 550 K, 1 h; (●) T_{red} 600 K, 1 h; (□) T_{red} 650 K, 1 h; (■) T_{red} 700 K, 1 h; (▲) T_{red} 750 H, 1 h; (△) T_{red} 750 K, 12 h.

of methyl acetate consumed. Beyond 650 K, significant decreases of the methane selectivity ensue from further increases of the reduction temperature. However, the effective methane selectivity decreases with increasing reduction temperature. For the reduction temperatures in excess of 650 K, the effective methane selectivity is only a function of the methyl acetate conversion, and a constant low level is attained. This is shown in Fig. 3b. High-temperature reduction has significantly lowered, i.e. improved, the methane selectivity.

3.3. *Ethane formation*

Ethane selectivity at varying reduction temperatures shows a pattern similar to the methane selectivity. In Fig. 4a, this is shown as a function of the reaction temperature. Generally, the ethane selectivity increases with increasing reaction

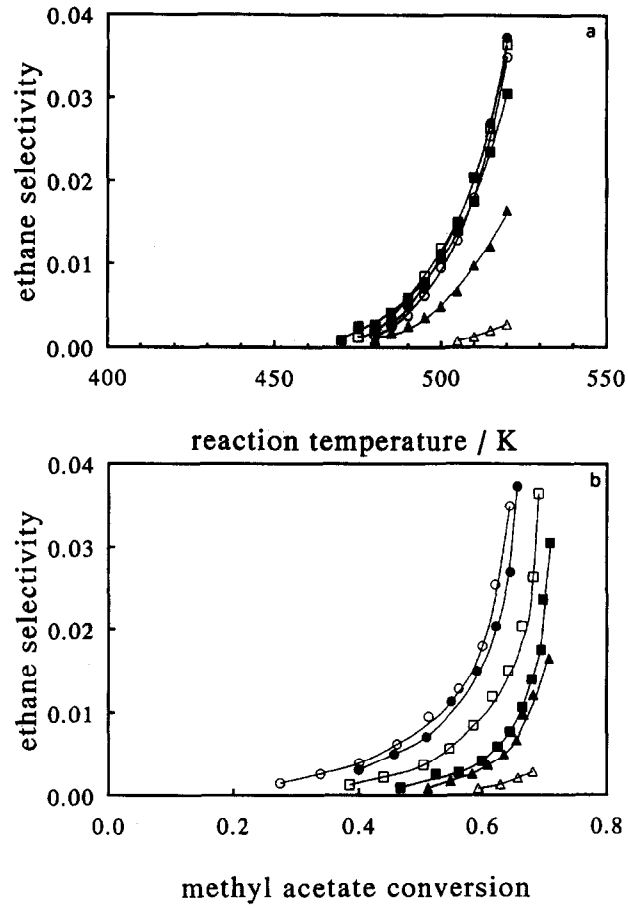

Fig. 4. (a) Effect of the reductive pretreatment. Ethane selectivity at varying reduction pretreatment versus the reaction temperature. (b) Effect of the reductive pretreatment. Effective ethane selectivity at varying reduction pretreatment versus the methyl acetate conversion. (○) T_{red} 550 K, 1 h; (●) T_{red} 600 K, 1 h; (□) T_{red} 650 K, 1 h; (■) T_{red} 700 K, 1 h; (▲) T_{red} 750 H, 1 h; (△) T_{red} 750 K, 12 h.

temperature. The ethane selectivity is independent of the reduction temperatures up to 700 K. Apparently, the ethane selectivity is only dependent on the reaction temperature. The independence of the reduction temperature infers that the consumption of methyl acetate and the production of ethane are directly connected. However, after reduction at 750 K, significantly lower selectivities to ethane are observed. If plotted versus the conversion (see Fig. 3b), significantly lower effective ethane selectivities are found at increasing severity of the reduction pretreatment. Hence, high-temperature reduction has markedly lowered both the *effective* methane and ethane selectivities and improved the catalyst performance in this respect.

3.4. Ethene formation

Ethene selectivity as a function of varying reduction temperature is comparable to the methane and ethane selectivities with respect to the dependency on the

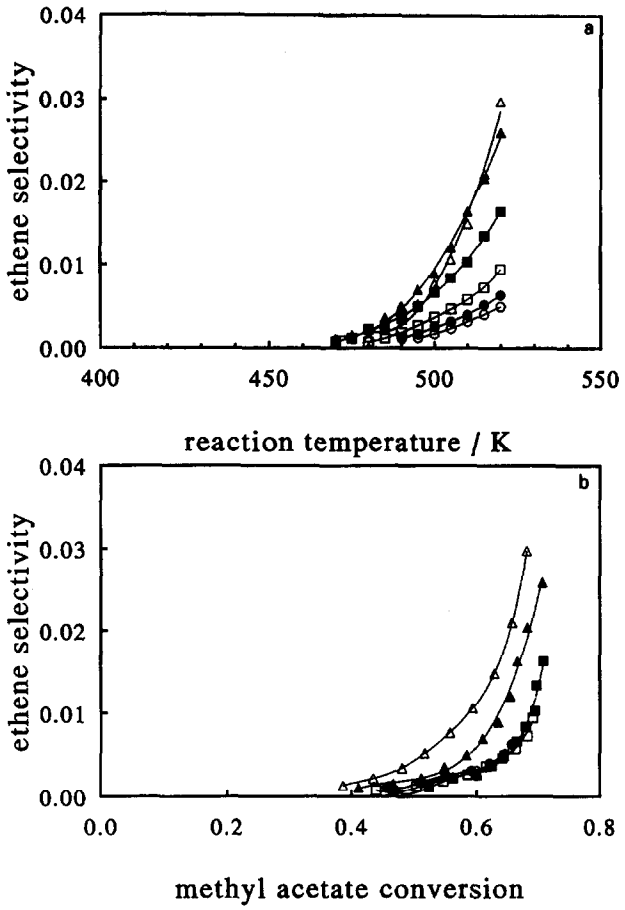

Fig. 5. (a) Effect of the reductive pretreatment. Ethene selectivity at varying reduction pretreatment versus the methyl acetate conversion. (b) Effect of the reductive pretreatment. Effective ethene selectivity at varying reduction pretreatment versus the methyl acetate conversion. (○) T_{red} 550 K, 1 h; (●) T_{red} 600 K, 1 h; (□) T_{red} 650 K, 1 h; (■) T_{red} 700 K, 1 h; (▲) T_{red} 750 H, 1 h; (△) T_{red} 750 K, 12 h.

reaction temperature, but remarkably different as a function of the reduction temperature. As is shown in Fig. 5a, the increase of the reduction temperature brings about an increase in the ethene selectivity. However, for reduction temperatures up to 700 K, the effective ethene selectivity (see Fig. 5b) is only dependent on the methyl acetate conversion, and not on the reaction temperature. A reduction temperature of 750 K even results in a higher effective ethene selectivity, which is possibly connected with a lower ethane selectivity (see Fig. 4b).

As a general observation in this and previous studies, when catalysts had been subjected to high temperatures, a white deposit was found at the reactor outlet. These deposits are readily soluble in diluted nitric acid. The presence of zinc and the absence of copper in this deposit were established by ICP/AES. The white deposit consists of zinc(II) acetate, which is volatile at the reaction temperatures (420 K–520 K), and/or of metallic zinc. Mar et al. [9] found sublimation of

Table 1
Copper and zinc metal assays of precursor and reduced samples of the $Cu/ZnO/SiO_2$ catalyst

	Weight fraction Cu (cg/g)	Weight fraction Zn (cg/g)	Cu/Zn ratio
Precursor	13.5	6.8	2.0
Reduced at 600 K, 1 h	14.8	7.3	2.1
Reduced at 750 K, 12 h, after complete cycle.	15.7	6.9	2.3

zinc(II) acetate at 507 K. Metallic zinc is volatile at reduction temperatures in excess of the melting temperature, 694 K [10]. In order to examine whether the deactivation after the reductions at 750 K is caused by a loss of zinc from the catalyst, the contents of zinc and copper in the spent catalyst were determined by ICP/AES. For comparison, also the copper and zinc contents of the precursor and a catalyst sample reduced at 600 K for one hour were analyzed. The results are shown in Table 1. After reduction at 750 K and completion of the cycle of activity measurements, the copper–zinc ratio is higher than after reduction at 600 K, most likely because of the evaporation of zinc from the catalyst.

In order to gain further insight in the effects of high-temperature reductions on the catalyst activity, several techniques were used for catalyst characterization. These include thermogravimetric analysis, determination of copper surface areas, X-ray diffraction, hydrogen chemisorption and FT-IR spectroscopy of chemisorbed carbon monoxide.

3.5. Thermogravimetric analysis/metal surface area

The significant effect of the high-temperature reduction on the $Cu/ZnO/SiO_2$ catalyst occurs in the last stage of the reduction. The relevant range between 550 K and 700 K is marked by the shaded area in the differential thermogravimetric profile in Fig. 6. The reduction maximum at 450 K is representative for copper-based catalysts, whereas the long tail is characteristic for the zinc-promoted catalyst; there is still a measurable rate of reduction at 750 K.

The degree of reduction as a function of the reduction temperature was determined thermogravimetrically. Fig. 7 illustrates the gradual increase of the degree of reduction with the rise of the reduction temperature. The fraction of reduced copper is 0.65 after reduction at 550 K, and is higher than the theoretical value 1 for reduction temperatures in excess of 700 K. Reduction at 750 K for 12 h results in an apparent degree of reduction of 1.24. This value corresponds with the reduction of approximately half of the zinc oxide present in the catalyst. Reduction of oxidic zinc is normally not possible at 750 K, but brass formation provides the driving force for the formation of zero-valent zinc [11]. Evaporation of zinc during the fifteen minutes of evacuation at the highest reduction temperatures is an additional contribution to the weight loss. The melting point of zinc is 694 K and sublimation of the liquid phase proceeds easily under vacuum.

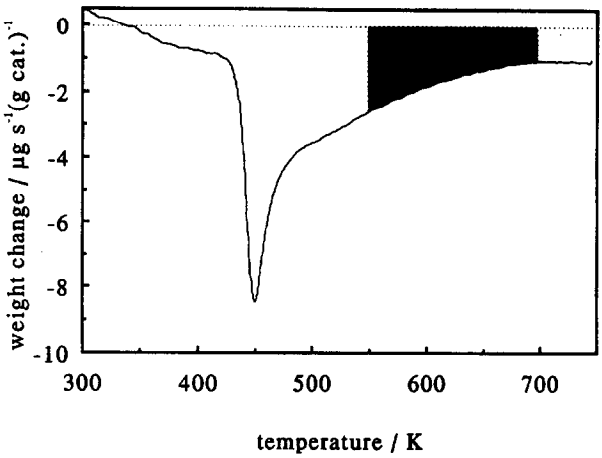

Fig. 6. Differential thermogravimetric profile of the 15 wt.-% Cu/9 wt.-% ZnO/SiO_2 catalyst. The heating rate was 0.02 K s^{-1}.

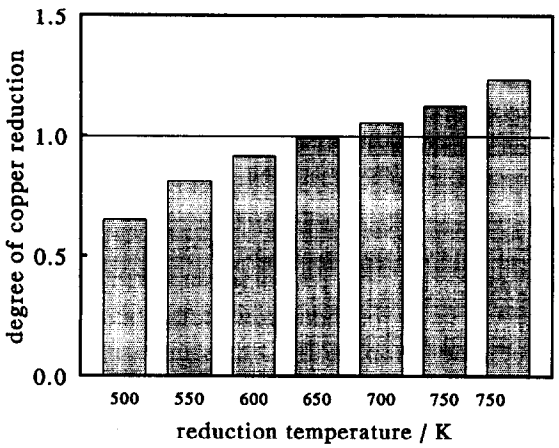

Fig. 7. The degree of reduction of the $Cu/ZnO/SiO_2$ catalyst as a function of the reduction pretreatment.

After each reduction step in the thermobalance, the copper surface area was measured by decomposition of nitrous oxide. The results are displayed in Fig. 8. The surface area is virtually constant and almost independent of the reduction temperature. The surface area has an initial value of 10.1 m^2 (g cat) $^{-1}$ after reduction at 500 K, but only a relatively small increase is observed to the maximum value of 12.7 m^2 (g cat.) $^{-1}$ after reduction at 650 K. At reduction temperatures in excess of 650 K, slightly lower values of the copper metal area were observed.

3.6. Determination of copper crystallite size

In X-ray diffraction (XRD) one broad peak is found at $2\theta = 43.4°$, for three different reduction pretreatments, which are shown in Table 2. With Cu Kα radiation, this is a diffraction line characteristic for fcc-copper. Using Bragg's law

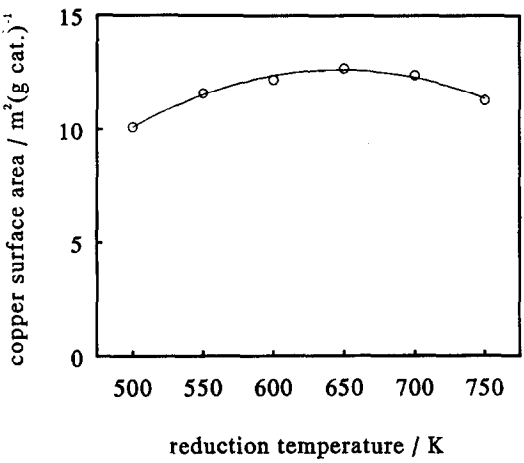

Fig. 8. Copper surface area of the $Cu/ZnO/SiO_2$ catalyst as a function of the reduction pretreatment.

[12], a lattice dimension of 0.3611 nm can be calculated. This value is in agreement with the lattice constant for pure metallic copper [13]. Guljaev and Trusova [14,15] reported that the copper lattice constant shifts to higher values if alloy formation between copper and small amounts of zinc occurs. This results in a smaller angle for the diffraction line. Since this shift was not observed, formation of brass can be excluded for the XRD-visible copper crystallites, even for the most severely reduced catalyst. Using the Scherrer equation [12], the size of the copper crystallites can be calculated from the width of the diffraction line. The crystallite size is apparently dependent on the pretreatment, as the mean particle size found after reduction at 700 K is larger than after reduction at 600 K. Moreover, after reduction at 600 K, a broad hump hardly surpassing the background was observed, but after reduction at 700 K a well-defined diffraction peak had developed. An identical well-defined peak was found after reduction at 750 K. Apparently, further sintering had not occurred. Finally, the X-ray spectra gave no indication of the presence of crystalline zinc oxide.

3.7. Hydrogen chemisorption

In order to establish the influence of the hydrogen coverage on the catalyst activity, hydrogen was chemisorbed at 500 K, which is a representative temperature for the reaction conditions. The results are shown in Fig. 9. High-temperature

Table 2
Crystal parameters from X-ray diffraction

Reduction pretreatment	2θ	d_p (XRD) (nm)
600 K, 1 h	43.4	2.8
700 K, 1 h	43.4	4.4
750 K, 12 h	43.4	4.5

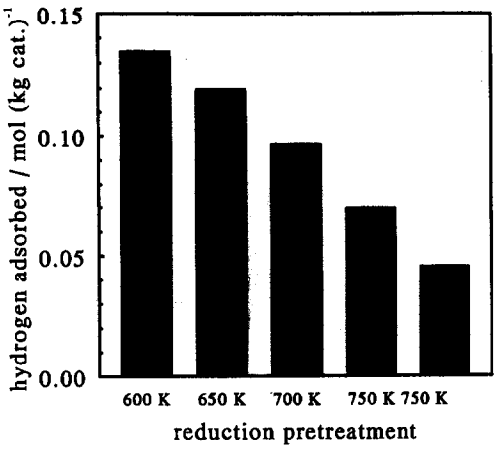

Fig. 9. Amounts of hydrogen chemisorbed at 500 K as a function of the catalyst reduction temperature.

reductions result in a lowering of the hydrogen uptake. The amount of hydrogen chemisorbed on the $Cu/ZnO/SiO_2$ catalyst decreases from 0.13 mol kg^{-1} after reduction at 600 K to 0.042 after reduction at 750 K for twelve hours. After the most severe reduction treatment, a considerable amount of bluish grey metallic zinc was found in the cold part of the glass reactor. Evacuation at 750 K largely causes the zinc evaporation.

3.8. Fourier-transform infrared spectroscopy of adsorbed carbon monoxide

In order to study the possible effects of high-temperature reductions on the surface morphology and the oxidation state of the $Cu/ZnO/SiO_2$ catalyst, FT-IR spectroscopy of adsorbed carbon monoxide was used, the method being well established for Cu/ZnO methanol synthesis catalysts [16–18]. Both adsorption and evacuation spectra were recorded.

Fig. 10 shows the adsorption spectra as a function of increasing severity of the reduction pretreatment. The spectra were recorded five minutes after exposure to 2 kPa of carbon monoxide. All the spectra are characterized by one single peak around 2100 cm^{-1}, which did not change in absorbance between five and 60 min of exposure time. With increasing severity of the reduction treatment the intensity of the absorption peak becomes lower. Concomitantly, the wave number shifts from 2113 cm^{-1} after reduction at 600 K for one hour to 2102 cm^{-1} after reduction at 750 K for twelve hours. Carbon monoxide associated with positively charged copper (Cu^+) is mostly found at 2124 cm^{-1} [18] and if bound to zero-valent copper at about 2100 cm^{-1} [19]. Hence, the red shift of the absorbance with increasing reduction temperature testifies of an increasing degree of reduction of the catalyst's copper surface.

Additional information on the state of the copper surface can be obtained from the evacuation spectra, as it is known that adsorbed carbon monoxide can be quickly

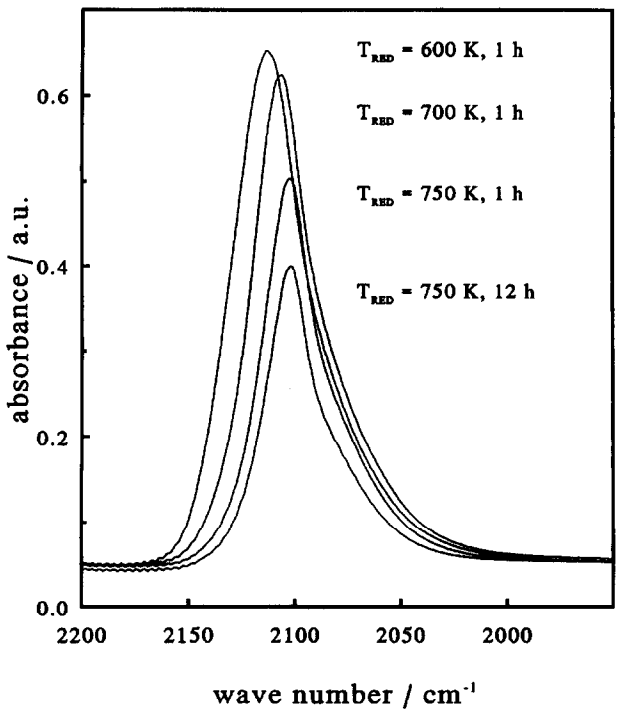

Fig. 10. FT-IR spectra of 2 kPa of carbon monoxide adsorbed on the $Cu/ZnO/SiO_2$ catalyst for four different reduction treatments.

removed from copper metal adsorption sites, but less easily from oxidized copper species [20]. Fig. 11 shows the spectra recorded immediately after the evacuation of 2 kPa of carbon monoxide. With increasing reduction severity, the peak shifts from 2121 cm^{-1} to 2106 cm^{-1} and its intensity becomes lower. This confirms the disappearance of positively charged copper sites. After reduction at 600 K and 700 K, the reduction is not yet complete, but after reduction at 750 K almost only zero-valent copper is present at the catalyst surface. The absence of adsorption bands at 2169 and 2178 cm^{-1} [17] infers that no crystalline zinc oxide is present in the catalyst.

3.9. Practical application of the high-temperature reduction

For ensuring optimum catalyst activity and selectivity, the preferred reduction temperature of the $Cu/ZnO/SiO_2$ catalyst is 700 K. However, this is too high a temperature for application in existing reactors for fatty alcohol synthesis, which have usually not been designed for high temperatures. High-temperature pretreatment in a dedicated unit can be a solution for this dilemma. After passivation of the pre-reduced catalyst, a low-temperature re-reduction should be sufficient for restoring the original catalyst activity.

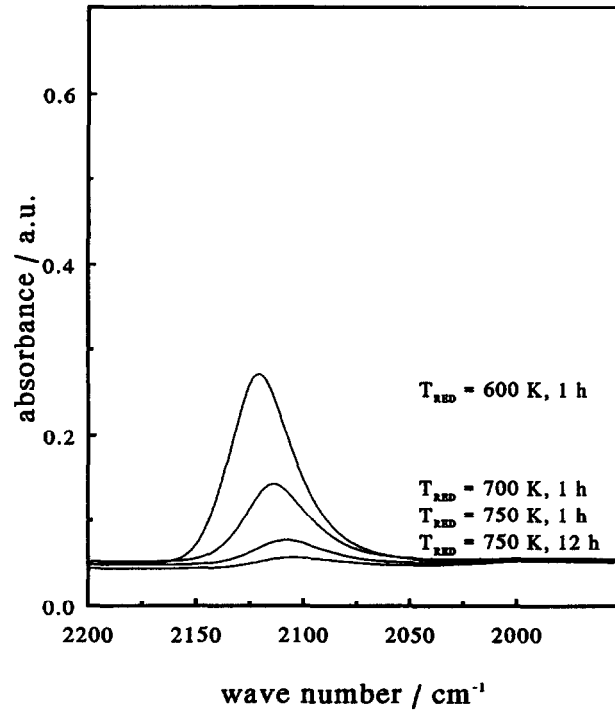

Fig. 11. FT-IR spectra of adsorbed carbon monoxide on the $Cu/ZnO/SiO_2$ catalyst for four different reduction treatments. Spectra were recorded immediately after evacuation of 2 kPa of carbon monoxide at a system pressure lower than 1 mPa.

In order to demonstrate the feasibility of this procedure, the sequence of high-temperature reduction, passivation and re-reduction was investigated in the micro-flow reactor. After calcination at 750 K, the $Cu/ZnO/SiO_2$ catalyst was first reduced

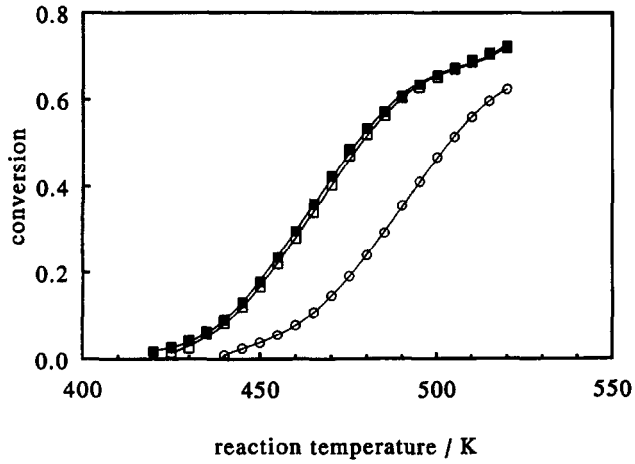

Fig. 12. The effect of low-temperature re-reduction (550 K) on the activity of a passivated $Cu/ZnO/SiO_2$ catalyst (□). For comparison: the activity after standard low-temperature reduction at 550 K (○) and the activity after high-temperature reduction at 700 K (■).

at 550 K for one hour. The catalyst activity after this standard low-temperature reduction was measured as a function of the reaction temperature, between 420 K and 520 K. Subsequently, the high-temperature reduction at 700 K was performed, followed by a second series of activity measurements. After the activity measurements, reaction intermediates were desorbed in hydrogen at 520 K, and the catalyst was carefully oxidized at 363 K in a pure nitrous oxide flow of 0.5 $cm^3\ s^{-1}$, during 30 min. The sample was cooled down to room temperature and subsequently exposed to an air flow of 1 $cm^3\ s^{-1}$ for sixteen hours. The re-reduction was conducted at 550 K for one hour. Finally, a third cycle of activity measurements was performed. Fig. 12 illustrates the feasibility of the passivation and low-temperature re-reduction. The original high activity of the pre-reduced catalyst can be re-obtained by low-temperature reduction after passivation and exposure to air. The evident advantages of the high-temperature reduction are therefore relevant to practical applications.

4. Discussion

The presence of the zinc oxide promoter in the $Cu/ZnO/SiO_2$ catalyst is of overriding importance in the activity increase by high-temperature reduction. We have found a remarkable difference with an unpromoted silica-supported copper catalyst, for which the activity holds constant over the range of reduction temperatures between 543 K and 743 K [21]. The method of catalyst preparation most likely has a decisive influence on the increase of the activity with increasing reduction temperature. Silica-supported copper catalysts prepared by homogeneous precipitation have been shown to be stable at high temperature [22]. In contrast, Cu/ZnO catalysts prepared by co-precipitation are not stable under reducing conditions at elevated temperatures. Using EXAFS, Tohji et al. [23] observed irreversible sintering of such a catalyst by reduction at 673 K. Accordingly, the method of catalyst preparation causes the stabilization of a specific copper–zinc interaction, which might otherwise have been destroyed by the high-temperature reduction.

Because of the remarkable activity increase and the stability at high temperature, the current catalyst system is very useful in the investigation of the copper–zinc interaction. The nature of this interaction has been the subject of a longstanding and controversial discussion, mainly in relation to the hydrogenation of carbon oxides and the water–gas shift reaction. Nevertheless, little is known yet about the significance of the copper–zinc oxide synergy for the hydrogenolysis of esters.

The activation energy of the reaction is 126 kJ mol^{-1} and constant over the range of reduction temperatures between 550 K and 700 K. Therefore, the activity increase with increasing reduction temperature most likely emanates from the creation of more active sites. If the additional active sites would have the same structure as the sites already present after low-temperature reduction, a constant turnover frequency

Table 3
Turnover frequencies of the $Cu/ZnO/SiO_2$ catalyst at varying reduction temperatures

Reduction pretreatment	Turnover frequency at 460 K (s^{-1})
1 h at 600 K	$1.2 \cdot 10^{-4}$
1 h at 700 K	$6.0 \cdot 10^{-4}$
12 h at 750 K	$4.6 \cdot 10^{-4}$

with increasing reduction temperature would be expected. However, the development of the turnover frequency is commensurate with the development of the catalyst activity, as the copper metal area shows only little dependence on the reduction temperature. Table 3 shows the turnover frequencies at 460 K, which were determined from steady-state activity measurements. The raising of the reduction temperature from 600 K to 700 K results in a five-fold increase of the turnover frequency. Hence, the increase of the turnover frequency indicates the formation of a different type of highly active sites after reduction at 700 K. Additionally, the deactivation after reduction at 750 K is reflected in a lower value of the turnover frequency. Part of the active sites has apparently been destroyed.

The existence of at least two different copper species is corroborated by the reduction behaviour. The differential thermogravimetric reduction profile in Fig. 6 is characterized by a maximum at 450 K and by a long tail in excess of this temperature. The peak stems from the reduction of Cu^{2+} which is mainly present in the silicate matrix. This reduction step presumably results in the formation of copper crystallites supported on silica. However, the retardation of the reduction with respect to the reduction of an unpromoted copper catalyst is caused by the presence of zinc in the catalyst [4]. The broad reduction band between 500 K and 750 K originates from the reduction of a copper species in close contact with the zinc-containing matrix. Finally, zinc reduction has been established for reduction temperatures in excess of 700 K. According to Van Herwijnen and De Jong [11], zinc reduction in the Cu/ZnO system may proceed at temperatures above 573 K, with the concomitant formation of brass.

Over the entire range of reduction temperatures copper crystallites of 3–5 nm are present in the catalyst. This has been established by X-ray diffraction. These crystallites expose active sites for the reaction, since unpromoted Cu/SiO_2 catalysts are also active in the hydrogenolysis of methyl acetate, the turnover frequency at 460 K being about $10^{-4}\ s^{-1}$ [4]. The much higher turnover frequency of the zinc-promoted catalyst after reduction at 700 K demonstrates the large contribution of the copper–zinc phase to the activity.

The importance of metallic copper in the active sites can be deduced from the increase of the degree of reduction between 600 K and 700 K. In the activity measurements, the methane and ethane selectivities as a function of the reaction temperature are independent of the pretreatment for reduction temperatures up to 650 K and 700 K, respectively (see the Figs. 3a and 4a). This constant proportionality between the methyl acetate consumption and the production of methane and

ethane, which is independent of the reduction temperature, indicates that the formation of methane and ethane proceeds on the same sites as the methyl acetate hydrogenolysis. With increasing reduction temperature, the higher number of active sites is responsible for the increase in the methane and ethane formation to the same extent as for the increase in the methyl acetate consumption. After reduction at 600 K, the active sites are largely located on copper crystallites having little interaction with the zinc promoter. After reduction at 700 K, the most active sites are in close contact with the zinc-containing phase. The identical selectivity pattern at the two reduction temperatures infers a certain similarity between the sites formed by the high-temperature reduction and those formed by the low-temperature reduction. Hence, the observed selectivities to methane and ethane suggest that all the active sites consist of ensembles of copper atoms. This is in line with Kohler et al. [24], who proposed that the hydrogenolysis reaction proceeds on copper metal in Cu/SiO_2 catalysts prepared by ion exchange.

In spite of the activity increase, the development of the copper surface area (see Fig. 8) does not point to a large increase of the number of active sites with increasing reduction temperature. The increase of the copper surface area as a result of the higher degree of reduction is counteracted by a certain agglomeration of the copper crystallites, which is suggested by X-ray diffraction. The number of copper sites formed by the high-temperature reduction is small, but these copper sites exhibit high activity for ester hydrogenolysis.

Concerning the nature of the copper–zinc oxide interaction, the joint increase of the activity and the degree of reduction suggests that positively charged copper species are not relevant to the active sites for the hydrogenolysis of methyl acetate. This is confirmed by the results of FT-IR spectroscopy, which have shown that the amount of carbon monoxide adsorbed on positively charged copper sites is much lower after reduction at 700 K than after reduction at 600 K. Since the additional sites formed by high-temperature reduction are not visible in XRD, whereas an enlarged copper metal surface has not been observed by nitrous oxide decomposition, clear evidence of the role of metallic copper is not provided by the current results. Hence, in view of the increase of the degree of reduction and the FT-IR results, the origin of the enhanced catalyst activity is thought to stem from the metal rather than from the copper(I) ions, although a minor charge transfer between the promoter and a highly active copper species cannot be excluded.

For the interaction in a Cu/ZnO catalyst reduced at 523 K, Klier [25] has presented a geometric model describing the contact between the zinc oxide (10$\bar{1}$0) plane and the copper (211) plane. Because of the absence of crystalline zinc oxide, which was established by X-ray diffraction and by FT-IR spectroscopy, an epitaxial interaction between copper and zinc oxide does not offer plausible explanations for the enhanced activity in the current catalyst system. However, the presence of zinc silicates might give rise to the formation of epitaxial copper layers. The formation of highly active copper sites for the reaction is thought to result from the interaction with the zinc-modified silica.

The development of the methane and ethane selectivities as a function of the reduction temperature suggests that the formation of these side products proceeds on copper sites. In contrast the selectivity to ethene behaves differently and increases with the reduction temperature (see Fig. 5a). The formation of ethene may proceed by dehydration of ethanol on acid sites at the catalyst surface. The calcined catalyst precursor contains mixed copper and zinc silicates. With increasing degree of reduction, divalent copper is reduced to copper metal and concomitantly, hydroxyl groups are formed at the silica surface [26]. These hydroxyl groups are thought to create surface acidity. The remarkable increase of the ethene formation after reduction at 750 K is consistent with this explanation, since the release of oxidic zinc from the silicate structure by reduction to metallic zinc yields even more hydroxyl groups.

The catalyst deactivation after reduction at 750 K results from the reduction of oxidic zinc and probably from the formation of brass. This mechanism of deactivation has also been proposed for the methanol synthesis and the water–gas shift reaction [11]. Siefering and Griffin [27] observed evaporation of metallic zinc from a zinc layer on copper foil at a temperature as low as 600 K. For the current catalyst system, possible zinc evaporation is confirmed by the analysis of the spent catalyst and by the weight loss in the thermobalance.

However, for the current catalyst system there is no direct evidence of a connection between brass formation and the deactivation. The considerable zinc reduction observed in the thermobalance after reduction at 750 K is not confirmed by the results of X-ray diffraction, which have shown the formation of copper crystallites. The occurrence of the zinc reduction is therefore an indication of brass formation in a copper phase which is not visible by X-ray diffraction. The presence of a finely dispersed copper phase is presumed.

Changes in the zinc-containing phase are also reflected in the results of the hydrogen chemisorption. The amounts of hydrogen shown in Fig. 9 represent the irreversible chemisorption of hydrogen, which is mostly associated with defect sites [28]. The lowering of the hydrogen chemisorption after high-temperature reduction therefore indicates a decrease of the number of oxygen vacancies. The ongoing reduction of oxidic zinc to metal with increasing reduction temperature presumably causes the loss of these defects.

Hydrogen spillover from zinc oxide to copper crystallites has been proposed as a possible explanation of the copper–zinc synergy in the methanol synthesis [29]. However, The development of the catalyst activity in the hydrogenolysis of methyl acetate is the reverse of the development of the hydrogen chemisorption with the reduction temperature. Although the hydrogen chemisorbed on the zinc-containing phase probably participates in the reaction it is not a key factor in the activity of the catalyst in the ester hydrogenolysis. The selectivity is affected to some extent, inasmuch as the low uptakes of hydrogen after reduction at 750 K coincide with the decreased formation of ethane (Figs. 4a and 4b) and the further increased formation of ethene (Figs. 5a and 5b). Apart from the effect of acid sites on the

ethene formation, the lower hydrogen coverage after high-temperature reduction may be connected with a decreased ethene consumption as a consequence of the reduced double-bond hydrogenation.

5. Conclusions

For a silica-supported copper–zinc catalyst prepared by homogeneous precipitation, remarkable increases in the activity for ester hydrogenolysis have been observed with increasing reduction temperatures up to 700 K. Further increase of the reduction temperature results in a deactivation. As for the occurrence of side reactions, the formation of methane and ethane is thought to proceed on copper metal sites; in contrast ethene is formed by dehydration of ethanol on acid sites, which develop with the increase of the degree of reduction.

The absence of a proportionality between the activity and the copper metal area has been established. This is assigned to the formation copper metal sites of different reactivity, the sites formed by high-temperature reduction being more active than those formed by low-temperature reduction. The presence of 3–5 nm copper crystallites and the absence of crystalline zinc oxide have been assessed. Catalyst deactivation proceeds if the reduction temperature exceeds the melting temperature of zinc. Evidence of zinc reduction and evaporation has been found at a reduction temperature of 750 K. Reduction of zinc is promoted by brass formation, but the effect of brass on the activity could not be determined.

It has been demonstrated that the advantage of the high-temperature reduction is relevant to practical applications. A $Cu/ZnO/SiO_2$ catalyst reduced at high temperature can be passivated, be contacted with air at room temperature, and subsequently be reactivated at a lower reduction temperature, whereby the high activity is retained. In addition to the higher catalyst activity, this results in a lower hydrogen consumption, lower water production and a lower exothermicity during the catalyst re-activation, enabling a quicker start-up procedure.

The enhanced activity may have significance not only for the hydrogenolysis of esters, but also for other industrially important reactions such as methanol synthesis, methanol decomposition, the water–gas shift reaction and the hydrogenation of aldehydes.

Acknowledgements

Prof. Dr. I.E. Wachs of Lehigh University is acknowledged for a useful discussion. We wish to thank Prof. Dr. H. Schenk and Mr. W. Molleman for the performance of the X-ray measurements and related discussions, Prof. Dr. A. Oskam and Mr. Th. Snoeck for the use of their FT-IR facilities, and Mr. J. Elgersma for the determination of the metal loadings in the catalysts.

References

[1] Fatty Alcohols: Raw materials, Methods, Uses, published by Henkel KGaA, Düsseldorf, 1981.
[2] R.A. Peters, in T.H. Applewhite (Editor), Proceedings of the World Conference on Oleochemicals, The American Oil Chemists' Society, Champaign, IL, 1991, pp. 181–188.
[3] F.Th. van de Scheur, J.J. Vreeswijk and L.H. Staal, in T.H. Applewhite (Editor), Proceedings of the World Conference on Oilseed Technology and Utilization, The American Oil Chemists' Society, Champaign, IL, 1993, pp. 453–457.
[4] F.Th. van de Scheur and L.H. Staal, Appl. Catal. A, 108 (1994) 63–83.
[5] R.G. Ackman, J. Chromatogr., 16 (1964) 173–179.
[6] M.-J. Luys, P.H. van Oeffelt, W.G.J. Brouwer, A.P. Pijpers and J.J.F. Scholten, Appl. Catal., 46 (1989) 161–173.
[7] J.W. Evans, M.S. Wainwright, A.J. Bridgewater and D.J. Young, Appl. Catal., 7 (1983) 75–83.
[8] J.W. Bijsterbosch, Ph.D. Thesis, University of Amsterdam, 1992.
[9] L.G. Mar, P.Y. Timbrell and R.N. Lamb, Thin Solid Films, 223 (1993) 341–347.
[10] R.C. Weast (Editor), The Handbook of Chemistry and Physics, 66th ed., CRC Press, Cleveland, Ohio.
[11] T. van Herwijnen and W.A. de Jong, J. Catal., 34 (1974) 209–214.
[12] H.P. Klug and L.E. Alexander, X-ray diffraction procedures, 2nd ed., Wiley, New York, 1973.
[13] W.B. Pearson, A Handbook of lattice spacings and structures of metals and alloys, Vol. 2, Pergamon Press, Oxford, 1965.
[14] A.P. Guljaev and E.F. Trusova, Zhurnal Tekhnicheskoi Fiziki 20(1) (1950) 66–78.
[15] A.P. Guljaev and E.F. Trusova, Structure Reports, 13 (1950) 103.
[16] E.R.A. Matulewicz, Ph.D. Thesis, University of Amsterdam, 1984.
[17] F. Boccuzzi, G. Ghiotti and A. Chiorino, Surf. Sci., 156 (1985) 933–942.
[18] F. Boccuzzi, G. Ghiotti and A. Chiorino, Surf. Sci., 183 (1987) L285–L289.
[19] J. Pritchard, T. Catterick and R.K. Gupta, Surf. Sci., 53 (1975) 1–20.
[20] N. Sheppard and T.T. Nguyen, Adv. Raman Infrared Spectr., 5 (1978) 67.
[21] F.Th. van de Scheur, B. van der Linden, M. Mittelmeijer-Hazeleger, J.G. Nazloomian and L.H. Staal, Appl. Catal., 111 (1994) 63–77.
[22] C.J.G. van der Grift, A.F.H. Wielers, B.P.J. Joghi, J. van Beijnum, M. de Boer, M. Versluis-Helder and J.W. Geus, J. Catal., 131 (1990) 178–189.
[23] K. Tohji, Y. Udagawa, T. Mizushima and A. Ueno, J. Phys. Chem., 89 (1985) 5671–5676.
[24] M.A. Kohler, N.W. Cant, M.S. Wainwright and D.L. Trimm, in M.J. Phillips and M. Ternan (Editors), Proc. 9th Int. Congr. Catalysis, Calgary, 1988, Vol. 5, The Chemical Institute of Canada, 1988, pp. 1043–1050.
[25] K. Klier, Appl. Surf. Sci., 19 (1984) 267–297.
[26] C.J.G. van der Grift, Ph.D. Thesis, University of Utrecht, 1989.
[27] K.L. Siefering and G.L. Griffin, Surf. Sci., 207 (1989) 525–538.
[28] G.J. Millar, C.H. Rochester, S. Bailey and K.C. Waugh, J. Chem. Soc. Faraday Trans., 89 (7) (1993) 1109–1115.
[29] R. Burch, S.E. Golunski and M.S. Spencer, J. Chem. Soc. Faraday Trans., 86 (15) (1990) 2683–2691.